The Usage of Two Dielectric Function Models*

Chen Hong and Shen Wenzhong†

(*Department of Physics, Shanghai Jiao Tong University, Shanghai* 200030, *China*)

Abstract: This paper presents an overview of the history, modifications, characteristics, and applications of two well known dielectric function models——the Forouhi-Bloomer model and the Tauc-Lorentz model——which have been widely used for the extraction and parameterization of optical constants in semiconductors and dielectrics. Based on analysis of their inherent characteristics and comparison via demonstrative examples, deeper and wider usage of the two models is predicted.

Key words: dielectric function models; optical constants; semiconductors
PACC: 7865; 7360F
CLC number: O484.4$^+$1 **Document code**: A **Article ID**: 0253-4177(2006)04-0583-08

1 Introduction

The optical constants (refractive index n and extinction coefficient k) of materials (either in bulk or thin film form) as functions of photon energy E (or wavelength λ) are important for both basic science and device applications. In general, the optical properties of any medium can be described by its complex refraction index, $N = n - ik$, or complex dielectric function, $\varepsilon = \varepsilon_1 - i\varepsilon_2$, where ε is related to N by $\varepsilon = N^2$, so that $\varepsilon_1 = n^2 - k^2$ and $\varepsilon_2 = 2nk$. The absorption coefficient α is directly related to k by $\alpha = 4\pi k/\lambda$. Optical constants can be extracted from optical transmission/reflection and spectroscopic ellipsometry measurements using various empirical formulas[1], effective-medium theories[2], or dielectric function models (DFMs)[3~6]. Of these approaches, DFMs are preferred in both extraction and parameterization of optical constants because of their Kramers-Kronig consistency and their convenient analytic representation of semiconductor dielectric responses.

Many DFMs have been established, including the well-known Forouhi-Bloomer (FB)[3], Tauc-Lorentz (TL)[4], Adachi[5,6], standard critical point[6], and damped harmonic oscillator models[6]. The latter three are relatively intricate and mainly apply to polycrystalline or crystalline semiconductors (especially compound semiconductors) with complex critical point structures. Compared to other DFMs, the FB and TL models are much simpler, as they have the fewest fitting parameters (only five). They are currently employed for several kinds of amorphous[3,4,7~10], polycrystalline[11~13], and crystalline/amorphous (c-/a-) mixed-phase semiconductor thin films[14,15]. The question arises whether these two models can be applied to other materials. In addition, the original TL model is directly related to the FB model[4]. The exploration and comparison of their characteristics are thus beneficial to their future applications. Although people frequently extract and parameterize optical constants with the FB and TL models, they pay little attention to the models' inherent characteristics and potential further applications.

In this paper, we investigate and summarize the history, modifications, inherent characteristics, and applications of the FB and TL models. We compare the two models and propose new viewpoints regarding their detailed applications. We predict deeper and wider usage of the two models.

* Project supported by the National Natural Science Foundation of China (No. 10125416) and the Shanghai Municipal Major Projects (Nos. 03DJ14003, 05DJ14003)

† Corresponding author. Email: wzshen@sjtu.edu.cn

Received 24 October 2005, revised manuscript received 16 January 2006

2 Forouhi-Bloomer model

In 1986, Forouhi and Bloomer proposed a theoretical formulation of optical constants for amorphous semiconductors and dielectrics[3]. With first-order time-dependent perturbation theory, they derived the following simple expressions for the optical constants:

$$k(E) = \frac{A_{FB}(E - E_{FB})^2}{E^2 - B_{FB}E + C_{FB}} \quad (1)$$

$$n(E) = n_\infty + \frac{B_0 E + C_0}{E^2 - B_{FB}E + C_{FB}} \quad (2)$$

where

$$B_0 = \frac{A_{FB}}{Q}\left(-\frac{B_{FB}^2}{2} + E_{FB}B - E_{FB}^2 + C_{FB}\right)$$

$$C_0 = \frac{A_{FB}}{Q}\left((E_{FB}^2 + C_{FB})\frac{B_{FB}}{2} - 2E_{FB}C_{FB}\right)$$

$$Q = \frac{1}{2}\sqrt{4C_{FB} - B_{FB}^2}$$

Equations 1 and 2 are consistent with Kramers-Kronig analysis. This FB model provides a physical picture of electronic transitions based on parabolic valence and conduction bands. The five fitting parameters are as follows: n_∞, the refractive index of the material at optical frequencies; E_{FB}, the optical gap in the FB model (referred to as the "FB gap" hereafter); A_{FB}, a constant that is proportional to the ratio of the square of the position matrix element to the lifetime of the electronic transitions; B_{FB}, twice the energy difference between the centers of the valence and conduction bands; and C_{FB}, a constant that depends on both A_{FB} and B_{FB}.

In 1994, McGahan *et al*.[16] modified the FB model by taking into account the states in the gap and/or nonparabolic bands. However, their modification adds complexity and more fitting parameters. Later, Davazoglou[17] assumed $k(E)$ in Eq. 1 to be zero or a positive constant when $E < E_{FB}$ in detailed use of the FB model. This is sometimes justified experimentally, since some materials are transparent below E_{FB} or exhibit additional absorption due to free carriers that are below E_{FB} and within the near-infrared(IR) region.

However, there is a shortcoming in the original FB model and the modified versions by McGahan *et al*.[16] and by Davazoglou[17], and that is the underestimation of band gap values. Thus the gap values determined by these FB models are significantly less than those obtained by other physical models[11,17] and are even unphysically negative in some cases[16]. Fortunately, the Tauc rule, which has been used very successfully for decades for gap evaluation in indirect-gap semiconductors, yields reasonable band gap values according to the relation[18]

$$\alpha(E) = \frac{B_a}{E}(E - E_{Tauc})^2 \quad (3)$$

where B_a is a constant and E_{Tauc} is the optical gap (denoted as the "Tauc gap" hereafter). The Tauc gap can be easily deduced from optical transmission spectra using linear extrapolation with what are called Tauc plots by the relation[18]

$$\left(-\frac{E}{d}\ln T_r\right)^{1/2} \propto (E - E_{Tauc}) \quad (4)$$

where d is the film thickness and T_r is the magnitude of transmission, if $T_r = \exp(-\alpha d)$ near the fundamental absorption edge. This extrapolation method is independent of the film thickness d. As typical evidence of the shortcoming of the FB model, we plot in Fig. 1 the experimental (solid curve) and calculated (dashed curve, labeled FB) room-temperature optical transmission spectrum in a wide spectral range of 500～2500nm by means of least-square analysis for a *c*-/*a*- mixed-phase B-doped hydrogenated nanocrystalline Si(nc-Si∶H)

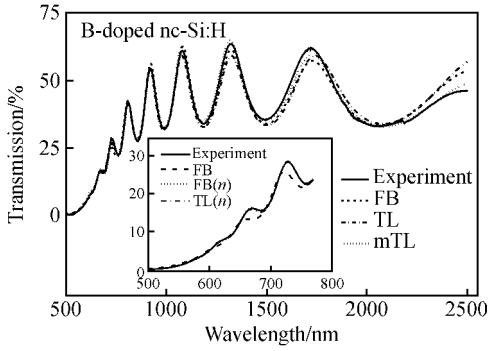

Fig. 1 Experimental optical transmission spectrum (solid curve) of B-doped nc-Si:H thin film[14] at room temperature, with the fitted results given by the FB (dashed curve), TL (dash-dotted curve) and mTL (dotted curve) models in the wide spectral range of 500～2500nm Shown in the inset is the same experimental spectrum (solid curve) in the narrow range of 500～770nm, with the fitted results by FB (dashed curve), FB(n) (dotted curve) and TL(n) (dash-dotted curve). Note that models used in the interband region only have been labeled with "n" in the parentheses.

thin film deposited on glass substrate[14], using

Eqs.(1) and (2) and the transmission equations presented in Ref.[18]. The fit by FB is good, but the yielded FB gap of 1.093eV is much smaller than the average Tauc gap of 1.494eV. The corresponding n and k are shown as dashed curves in Fig.2.

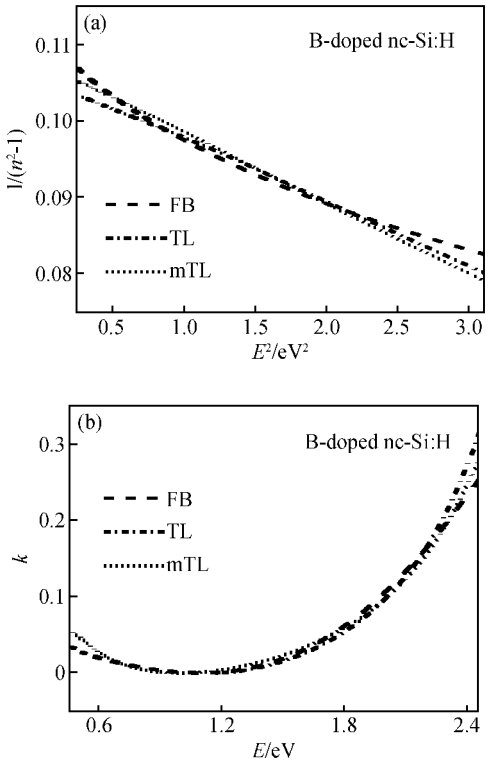

Fig.2 (a) Plots of factor $(n^2-1)^{-1}$ versus E^2 for the subgap refractive indices n; (b) Extinction coefficients k calculated by the FB (dashed curves), TL (dash-dotted curves) and mTL (dotted curves) models for the B-doped nc-Si∶H of Fig.1

Interband transitions cannot result in optical absorption for $E<E_{FB}$[3,4], while $k(E)>0$ for $E<E_{FB}$ according to Eq.(1). Therefore, the FB gap is an average effective gap which may even be negative if the FB model is used in a wide spectral range that includes both the above-band-gap and the below-band-gap regions. Moreover, it is implicit within Eq.(1) that it is closely comparable to the Tauc rule in the interband region (i.e., $E>E_g$ where E_g is the true optical gap). As a result, the FB model can be applied in the interband region (denoted as FB(n)). The feasibility of FB(n) is illustrated in the inset of Fig.1, where FB(n) (dotted curve) accurately reproduces the experimental spectrum in the narrow spectral range of 500～770nm, revealing a more reasonable FB gap of 1.502eV, in contrast to the FB gap of 1.093eV for the wide spectral region of 500～2500nm (dashed curve). Therefore, the FB model used in the interband region (i.e., FB(n)) yields reliable optical gaps (i.e., an accurate approximation of the true optical gaps) and optical constants. This presents a new viewpoint for the application of the FB model.

The FB(n) model is superior to the Tauc rule in the investigation of thermal effects on optical band gaps as well as optical constants in the interband region, as demonstrated by a typical p-type nc-Si∶H example[14]. This can be well understood as follows. First, there is some uncertainty in the linear extrapolation of Tauc gap values for different spectral ranges. In other words, it is difficult to determine the exact linear region of the experimental spectra that is suitable for linear extrapolation at a given temperature. This results in deviations of the Tauc gap values and eventually a smearing out of the thermal behavior of the true band gaps with the variation of temperature[19]. Second, the optical constants cannot be calculated by the above Tauc rule alone, since the dispersion equation for nc-Si∶H in the interband region is unknown. Finally, there are only five fitting parameters in the FB model, alleviating the problem of more fitting parameters inducing more uncertainty in the fitting procedure, particularly for temperature-dependent investigation.

There are several inherent shortcomings in the FB model and its variations[4]:

(1) In the original FB formulation, $k(E)>0$ for $E<E_{FB}$, which is unreasonable for undoped semiconductors. After all, many glasses are transparent. This was recognized by McGahan *et al*.[16] and Davazoglou[17].

(2) The original FB and its variations have $k(E)\rightarrow$ constant when $E\rightarrow\infty$; both experimental and theoretical results clearly indicate that $k(E)$ goes to 0 as $1/E^3$ or faster when $E\rightarrow\infty$. This limit is particularly important for Kramers-Kronig integration.

(3) The original FB and its variations use Kramers-Kronig integration from $-\infty$ to $+\infty$ to calculate $n(E)$ but do not incorporate time-reversal symmetry, which requires $k(-E)=-k(E)$.

Despite the above fundamental problems, the original FB model and its variations can extract or parameterize optical constants of matter ranging

from amorphous[3,7] or polycrystalline[11] to *c*-/*a*-mixed-phase(e. g., nc-Si ∶ H of Fig. 1) semiconductors and dielectrics. Finally, it is worth noting that the preceding statements are related only to the single FB model and that the original FB model has been extended for use in crystalline semiconductors (i. e. crystalline Si(c-Si)) and dielectrics by a multiple formalism (i. e., the superposition of several single-FB terms)[20].

3 Tauc-Lorentz model

In 1996, to overcome the above listed shortcomings in the FB model, Jellison and Modine proposed the empirical TL model for amorphous semiconductors and insulators[4]. The imaginary part of the dielectric function $\varepsilon_{2\mathrm{TL}}(E)$ is established by multiplying the Tauc joint density of states by the ε_2 obtained from the classical Lorentz oscillator model[4]:

$$\varepsilon_{2\mathrm{TL}}(E) = 2n(E)k(E) = \begin{cases} \dfrac{A_{\mathrm{TL}}E_{0\mathrm{TL}}C_{\mathrm{TL}}(E-E_{\mathrm{TL}})^2}{(E^2-E_{0\mathrm{TL}}^2)^2+C_{\mathrm{TL}}^2E^2}\times\dfrac{1}{E}, & E>E_{\mathrm{TL}} \\ 0, & E\leqslant E_{\mathrm{TL}} \end{cases} \tag{5}$$

The real part of the dielectric function $\varepsilon_{1\mathrm{TL}}(E)$ is obtained by Kramers-Kronig integration, and is given by

$$\varepsilon_{1\mathrm{TL}}(E) = \varepsilon_{1\infty} + \frac{2}{\pi}P\int_{E_{\mathrm{TL}}}^{\infty}\frac{\xi\varepsilon_{2\mathrm{TL}}(\xi)}{\xi^2-E^2}\mathrm{d}\xi \tag{6}$$

where P stands for the Cauchy principal part of the integral. Note that the integral is taken over positive energies, so the above-mentioned time-reversal symmetry property need not be considered. This integral can be solved in closed form as given by Eq. (6) of Ref. [4]. There are five fitting parameters in the above single TL model: the transition-matrix-element related A_{TL}, transition energy $E_{0\mathrm{TL}}$, a broadening parameter C_{TL}, the band gap E_{TL} (TL gap), and the constant $\varepsilon_{1\infty}$. The multiple TL model, which is the superposition of several single-TL terms, e. g., double TL(2TL)[12,13], generally corresponds to multi-transitions.

As indicated by Eq. (5), the TL model includes only interband transitions; any defect absorption, intraband absorption, or Urbach tail absorption is ignored. Four variations of the TL model have been proposed to remedy some of its limitations.

In 2002, Ferlauto *et al*. modified the TL model to include of the exponential Urbach tail(a variation we will denote as the TLU model)[21]. The TLU model seems more physically reasonable, and it introduces three additional fitting parameters. Later, Foldyna *et al*. extended the TLU model by assuming a continuous first derivative of the dielectric function[22]. In this case, there are only six fitting parameters. In 2003, Nguyen *et al*. proposed a generalized TL(GTL) model[23], of which the TL model is a special case. Very recently, we empirically modified the TL model by extending the non-zero part of $\varepsilon_{2\mathrm{TL}}(E)$ to the whole spectral range[24] without changing the expression of $\varepsilon_{1\mathrm{TL}}(E)$ (this modified version is denoted as "mTL" hereafter), in order to include free carrier absorption and obtain a more reliable below-band-gap refractive index for doped semiconductors such as B-doped nc-Si ∶ H. The mTL does not induce any additional fitting parameters.

It can be inferred from Eq. (5) that the original TL model used in a wide experimental spectral range covering both the region of transparency (or weak absorption) and the interband region will yield almost the same fitting parameters as those of the TL model used only in the interband region (denoted as TL(n)). For example, we also plot in Fig. 1 and its inset the TL-(500～2500nm, dash-dotted curve) and TL(n)-(500～770nm, dash-dotted curve) calculated transmission spectra of B-doped nc-Si ∶ H, respectively. The TL fit is good except in the weak absorption region of 1750～2500nm (where free carrier absorption causes a small decrease in the experimental transmission minimum), and the TL(n) reproduces the experimental data as well as FB(n), with the fitting parameters A_{TL}, C_{TL}, $E_{0\mathrm{TL}}$, E_{TL}, $\varepsilon_{1\infty}$ of 55.449eV, 0.543eV, 3.295eV, 1.145eV, 4.028 for TL and 55.369eV, 0.743eV, 3.418eV, 1.180eV, 4.746 for TL(n). Both TL gap values-1.145eV for TL and 1.180eV for TL(n)-are much smaller than the corresponding Tauc gap of 1.494eV. The TL gap is thus a mathematical gap rather than a real physical one, owing to the empirical nature of the TL model. This is because the components of the Lorentz oscillator and Tauc joint density of states in $\varepsilon_{2\mathrm{TL}}(E)$ may be suitable for describing the below-band-gap and above-band-gap absorption, respectively. The tradeoff between these two components results in a smaller nominal band gap E_{TL}

(TL gap) than the true optical band gap E_g, when the TL model fits real data. Hence the absorption below E_g is actually embodied within the photon energy range between E_{TL} and E_g. It is no wonder that the single or multiple TL models without any modifications are usually capable of reproducing the experimental data very well even below the optical band gap (see Refs. [4,9,12,13] for supporting examples).

Nevertheless, when free carrier absorption appears in the near-IR region for doped materials, TL overestimates n in this spectral range (see the TL fitting in 1500～2500nm of Fig. 1) since $k(E)$ is fixed at 0 for $E \leqslant E_{TL}$. Fortunately, we can resort to mTL to derive reliable optical constants, especially for the below-band-gap refractive index for doped samples. Its reliability is evidenced by the satisfactory fit (dotted curve) in Fig. 1, with the fitting parameters A_{TL}, C_{TL}, E_{0TL}, E_{TL}, $\varepsilon_{1\infty}$ of 54.889eV, 0.410eV, 3.312eV, 0.996eV, 2.751. The relevant $n(E)$ and $k(E)$ by mTL, shown as dotted curves in Fig. 2, are close to those yielded by FB (dashed curves) and TL (dash-dotted curves). The $n(E)$ of B-doped nc-Si:H obtained by mTL is smaller than that given by TL in the low energy region, which is justified since the calculated transmission extremes by mTL are blue shifted from those by TL (see the spectral simulation in 1500～2500nm of Fig. 1). The yielded $k(E)$ by mTL within the range of 0.5～1.0eV in Fig. 2 shows the trend of the free carrier absorption effect, indicating that the free carrier absorption increases with decreasing photon energy. Similar phenomena regarding free carrier absorption have also been reported in heavily doped polycrystalline silicon[25]. The mTL model is also workable for other B-doped nc-Si∶H deposited under different growth conditions (not shown here). As a result, we conclude that mTL is superior to TL for doped samples.

The "subgap" (mainly below E_g, sometimes below E_{0TL}) refractive index revealed by mTL or TL (in the single or multiple form) for large groups of matter, including B-doped nc-Si∶H (Fig. 2(a)), glass[8], hydrogenated amorphous carbon (a-C∶H)[9], a-SiN∶H[10], high-k dielectric HfO_2[12], and ferroelectric $Bi_{3.25}La_{0.75}Ti_3O_{12}$ (BLT)[13] (see also Fig. 3), are all found to obey the one-oscillator Wemple-DiDomenico (WD) model of the form[26]

$$n^2(E) - 1 = E_d E_0/(E_0^2 - E^2) \qquad (7)$$

where E_0 is the single oscillator energy, and E_d is the dispersion energy. Experimental verification of Eq. (7) can be obtained by plotting $1/(n^2-1)$ versus E^2, as shown in Figs. 2(a) and Fig. 3. The resulting straight lines yield values of the parameters E_0 and E_d. For instance, E_0 and E_d for the mTL-yielded subgap $n(E)$ (within the range of 0.50～1.58eV) of the B-doped nc-Si∶H in Fig. 2 are 3.412 and 31.687eV, respectively. In contrast, the FB-yielded subgap $n(E)$ cannot be well described by the WD model, as confirmed by another typical example of glass in Fig. 3, whose TL-yielded subgap $n(E)$ turns out to be consistent with its nature[27]. It should be noted that the complete expression of $\varepsilon_{1TL}(E)$ remains unchanged between mTL and TL. The refractive-index behavior's strict obedience of the WD model in the subgap region is thus believed to be inherent within the TL model and not the FB model.

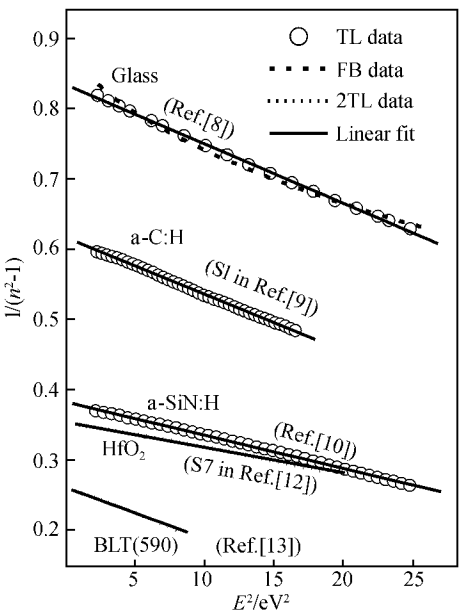

Fig. 3　Plots of factor $(n^2-1)^{-1}$ versus E^2 for the subgap refractive indices n (open circles: single TL model; dashed curves: FB model; dotted curves: double TL model; solid lines: linear fits) of various semiconductors and dielectrics

It is also a new finding that the subgap refractive index revealed by the TL model is strongly related to the one-oscillator WD model if the TL model is fitted to real data, no matter which kind of TL model is used (i.e., in a single or mul-

tiple form, or mTL) and regardless of the form of the investigated materials (i.e., amorphous, polycrystalline, or *c*-/*a*- mixed-phase). Then we are able to infer the following. In general, the single TL corresponds to one dominant interband optical transition, the double TL corresponds to two transitions, and so on. Since the single TL model is related to the single-oscillator WD model, and the multiple-oscillator WD model has been demonstrated to be equivalent to a one-effective-oscillator WD model[26], any multiple TL model is related to the single-oscillator WD model.

The reason the TL model is strongly related to the WD model is twofold. First, the TL model reveals a more reliable dielectric response than the FB model in the subgap region, where the refractive-index behavior of large groups of matter obeys the Sellmeier equation of the form $n^2(E) - 1 = (A_0 - 1) + B_0/(C_0^2 - E^2)$ with A_0, B_0 and C_0 as fitting constants. E^2 is generally much less than C_0^2 in the subgap region, and the Sellmeier equation is thus approximately equivalent to the WD expression according to the relation $(A_0 - 1) + B_0/(C_0^2 - E^2) \approx ((A_0 - 1)C_0^2 + B_0)/(C_0^2 - E^2)$. Second, when $E < E_g$ or when E_{TL} enough smaller than E, the TL model approaches the classical Lorentz oscillator model of the form[28]

$$\varepsilon_L(E) = \varepsilon_\infty + \frac{A_L}{E_{0L}^2 - E^2 - iC_L E} \tag{8}$$

whose expression for the real part of the dielectric function $\varepsilon_{1L}(E)$ turns out to be equivalent to the Sellmeier equation and subsequently to the WD expression after using $\varepsilon_1(E) = n^2(E)$ and neglecting the broadening term C_L. The other parameters are the constant ε_∞, amplitude A_L and band gap E_{0L}. We adopt the WD model here rather than the Sellmeier equation, because the WD parameters have fundamental physical significance and can provide new insight into the microstructure of matter[26].

In combination with the WD model, we can attach new physical significance to the transition energy parameter E_{0TL} of the TL model. E_0 is the energy of the effective oscillator, which is typically near the main peak of the imaginary part of the dielectric function ε_2. It has been extended to measure the energy difference between the "centers of gravity" of the valence and conduction bands, which is indicative of an average gap of the material[19]. This average gap gives quantitative information about the "overall" band structure, differing from the conventional optical gap such as Tauc gaps[14] which probes optical properties near the fundamental band gap of the material. In the successful usage of the single TL model (usually for amorphous, sometimes for *c*-/*a*- mixed-phase materials), the transition energy parameter E_{0TL}, which is closely comparable to E_0 and the peak energy of ε_2, reflects such overall band structure information. For example, $E_{0TL} = 3.312$eV and $E_0 = 3.412$eV for the B-doped nc-Si∶H by mTL in Fig. 1. In cases of the multiple TL model (generally for multi-transition amorphous, polycrystalline materials), multiple E_{0TL} parameters correspond roughly to different transition energies, or even critical points such as E_1; however, we can still resort to E_0 for the aforementioned "overall" band structure information, which may be further related to the specific bond density of matter[29].

Based on the relation between WD and TL, another criterion is proposed for judging whether the quantum size effect (QSE) is prominent within *c*-/*a*- mixed-phase materials such as B-doped nc-Si∶H (where Si nanocrystals are embedded in an amorphous Si matrix) from the viewpoint of $\varepsilon_1(E)$: the decrease in the subgap refractive index of the material is primarily ascribed to the average gap E_0 expansion, which proves to be equivalent to the method of Ref. [30]. When E_0 is larger than that of c-Si (i.e., 4.0eV, see Ref. [26]) it implies prominent QSE. Otherwise it implies negligible QSE. E_{0TL} of the single TL model also reveals similar qualitative information about QSE, since it approximates E_0. This criterion gives us a straightforward and convenient way to judge the degree of QSE from either E_0 or E_{0TL}. For instance, $E_{0TL} = 6.508$eV and $E_0 = 7.902$eV for the intrinsic nc-Si∶H[15]. Both of these values are significantly different from that of c-Si, which is an indication of QSE. This is reasonable since the grain size of the intrinsic nc-Si∶H is only about 3.5nm, less than the usual size limit of 5nm for considerable QSE in nc-Si∶H.

Mass density and information about coordination number can also be deduced from the TL fitting parameters in conjunction with the WD model. The parameter E_d, which is a measure of the strength of interband optical transitions and is

nearly independent of E_0, is found to follow the simple relationship $E_d = \beta N_c Z_a N_e$ in a variety of crystalline covalent and ionic solids and liquids. N_c is the coordination number of the cation nearest neighbor to the anion, and Z_a, N_e, β are constants[26]. In a diamond-type structure of c-Si, $N_c = 4$ with $E_0 = 4.0$eV and $E_d = 44.4$eV. The WD model was extended to amorphous semiconductor and glasses[27], by the proposed relation $E_d^a/E_d^x = (\rho^a/\rho^x)(N_c^a/N_c^x)$, where ρ is the mass density, and a and x refer to amorphous and crystalline forms, respectively. This relation is also expected to hold for mixed-phase materials like nc-Si∶H, with the possible distinction of constant β. Therefore, E_d mainly reveals information about density and coordination number (see Ref. [29] for supporting examples).

Finally, similar to the FB model, which has been successfully extended to crystalline semiconductors and dielectrics[20], we can also predict that the (single or multiple) TL model may be applicable for the optical characterization and microstructure investigation of many other covalent and ionic materials, including more than 100 widely different solids and liquids presented in Refs. [26] and [27], whether fully or partially crystalline and amorphous, provided the refractive-index dispersion behavior of these materials falls into the pattern described by the WD model and their subgap optical absorption is adequately small.

4 Further discussion

In addition to the above investigations of the FB and TL models, we give an overview of the characteristics and applications of these two models:

Although the FB and TL models can be used in the near IR to ultraviolet spectral range, only FB(n), and not TL(n), can yield reliable optical gaps of the material being studied. The TL gap is a mathematical one that is due to the empirical nature of the TL model, while the true band gap can be derived from the TL-yielded $k(E)$ by means of methods such as a Tauc plot. When fitted to real data, the TL model can yield more reliable optical constants ($n(E)$ and $k(E)$) than the FB model, especially the subgap $n(E)$. The TL-yielded subgap refractive index is found to be strongly related to the WD model, on the basis of which we can gain insights into the microstructure of matter and extend the applications of the TL model. Nevertheless, we think that the FB and TL models are not applicable to all kinds of semiconductors or insulators, but mainly to amorphous ones, since they were originally proposed for amorphous materials. Both can be extended to be applied in multiple forms for polycrystalline or crystalline materials. When the FB and TL models (or their modified versions) are not workable for specific substances with complex critical point structures or in the case of other spectral (e.g., far-IR) regions, one may resort to other DFMs, including the Adachi model[5,6] or the classical Drude model for reasonable determination of the optical constants.

5 Conclusions

The history, modifications, characteristics and applications of the well-known FB and TL dielectric function models have been investigated. Comparison is made between these two models using typical examples. New perspectives in the inherent characteristics of the two models are also proposed, which will facilitate their deeper and wider usage in many other semiconductors and insulators.

References

[1] Swanepoel R. Determination of the thickness and optical constants of amorphous silicon. J Phys E, 1983, 16: 1214

[2] Aspnes D E, Theeten J B, Hottier F. Investigation of effective-medium models of microscopic surface roughness by spectroscopic ellipsometry. Phys Rev B, 1979, 20: 3292

[3] Forouhi A R, Bloomer I. Optical dispersion relations for amorphous semiconductors and amorphous dielectrics. Phys Rev B, 1986, 34: 7018

[4] Jellison G E Jr, Modine F A. Parameterization of the optical functions of amorphous materials in the interband region. Appl Phys Lett, 1996, 69: 371

[5] Adachi S. Model dielectric function of hexagonal CdSe. J Appl Phys, 1990, 68: 1192

[6] Djurišić A B, Chan Y, Li E H. Progress in the room-temperature optical functions of semiconductors. Mat Sci Eng R, 2002, 38: 237

[7] Shen Weidong, Liu Xu, Zhu Yong, et al. Determination of optical constants and thickness of semiconductor thin films by transmission measurement. Chinese Journal of Semiconductors, 2005, 26(2): 335 (in Chinese) [沈伟东, 刘旭, 朱勇, 等. 用透过率测试曲线确定半导体薄膜的光学常数和厚度. 半

导体学报,2005,26(2):335]
[8] Kildemo M, Ossikovski R, Stchakovsky M. Measurement of the absorption edge of thick transparent substrates using the incoherent reflection model and spectroscopic UV-visible-near IR ellipsometry. Thin Solid Films, 1998, 313/314:108
[9] Hayashi Y, Yu G, Rahman M M, et al. Determination of optical properties of nitrogen-doped hydrogenated amorphous carbon films by spectroscopic ellipsometry. Appl Phys Lett, 2001, 78:3962
[10] Jellison G E Jr, Merkulov V I, Puretzky A A, et al. Characterization of thin-film amorphous semiconductors using spectroscopic ellipsometry. Thin Solid Films, 2000, 377/378:68
[11] Davazoglou D, Kouvatsos D N. Study of the electronic structure of amorphous and crystallized low pressure chemically vapor deposited silicon films near the absorption threshold. J Appl Phys, 2002, 92:4470
[12] Cho Y J, Nguyen N V, Richter C A, et al. Spectroscopic ellipsometry characterization of high-k dielectric HfO_2 thin films and the high-temperature annealing effects on their optical properties. Appl Phys Lett, 2002, 80:1249
[13] Hu Z G, Ma J H, Huang Z M, et al. Dielectric functions of ferroelectric $Bi_{3.25}La_{0.75}Ti_3O_{12}$ thin films on Si(100) substrates. Appl Phys Lett, 2003, 83:3686
[14] Chen H, Shen W Z. Temperature-dependent optical properties of B-doped nc-Si∶H thin films in the interband region. J Appl Phys, 2004, 96:1024
[15] Amans D, Callard S, Gagnaire A, et al. Ellipsometric study of silicon nanocrystal optical constants. J Appl Phys, 2003, 93:4173
[16] McGahan W A, Makovicka T, Hale J, et al. Modified Forouhi and Bloomer dispersion model for the optical constants of amorphous hydrogenated carbon thin films. Thin Solid Films, 1994, 253:57
[17] Davazoglou D. Optical properties of SnO_2 thin films grown by atmospheric pressure chemical vapor deposition oxidizing $SnCl_4$. Thin Solid Films, 1997, 302:204
[18] Chen H, Gullanar M H, Shen W Z. Effects of high hydrogen dilution on the optical and electrical properties in B-doped nc-Si∶H thin films. J Cryst Growth, 2004, 260:91
[19] Solomon I, Schmidt M P, Sénémaud C, et al. Band structure of carbonated amorphous silicon studied by optical, photoelectron, and X-ray spectroscopy. Phys Rev B, 1988, 38:13263
[20] Forouhi A R, Bloomer I. Optical properties of crystalline semiconductors and dielectrics. Phys Rev B, 1988, 38:1865
[21] Ferlauto A S, Ferreira G M, Pearce J M, et al. Analytical model for the optical functions of amorphous semiconductors from the near-infrared to ultraviolet: applications in thin film photovoltaics. J Appl Phys, 2002, 92:2424
[22] Foldyna M, Postava K, Bouchala J, et al. Model dielectric function of amorphous materials including Urbach tail. Proc SPIE, 2004, 5445:301
[23] Nguyen N V, Han J P, Kim J Y, et al. Optical properties of jet-vapor-deposited TiAlO and HfAlO determined by vacuum ultraviolet spectroscopic ellipsometry. AIP Conf Proc, 2003, 683:181
[24] Chen H, Shen W Z. Optical characterization of boron-doped hydrogenated nanocrystalline Si: H thin films. Surf Coat Technol, 2005, 198:98
[25] Mishina Y, Hirose M, Osaka Y. Optical determination of mobility and carrier concentration in heavily doped polycrystalline silicon. J Appl Phys, 1980, 51:1157
[26] Wemple S H, DiDomenico M Jr. Behavior of the electronic dielectric constant in covalent and ionic materials. Phys Rev B, 1971, 3:1338
[27] Wemple S H. Refractive-index behavior of amorphous semiconductors and glasses. Phys Rev B, 1973, 7:3767
[28] Zollner S, Demkov A A, Liu R, et al. Optical properties of bulk and thin-film $SrTiO_3$ on Si and Pt. J Vac Sci Technol B, 2000, 18:2242
[29] Chen H, Shen W Z. Perspectives in the characteristics and applications of Tauc-Lorentz dielectric function model. Eur Phys J B, 2005, 43:503
[30] Chen T P, Liu Y, Tse M S, et al. Dielectric functions of Si nanocrystals embedded in a SiO_2 matrix. Phys Rev B, 2003, 68:153301

两个介电函数模型的用法*

陈 红 沈文忠†

(上海交通大学物理系,上海 200030)

摘要:回顾了两个著名的广泛用于提取或参数化半导体和电介质材料光学常数的介电函数模型,即 Forouhi-Bloomer 和 Tauc-Lorentz 模型的历史、各种改进、各自特点和应用.在揭示它们内在特点和比较运用在具体实例的基础上,拓展和预言了这两个模型更为深入的和更为广泛的应用.

关键词:介电函数模型;光学常数;半导体
PACC:7865;7360F
中图分类号:O484.4+1 **文献标识码**:A **文章编号**:0253-4177(2006)04-0583-08

* 国家自然科学基金(批准号:10125416)和上海市重大基础研究计划(批准号:03DJ14003,05DJ14003)资助项目
† 通信作者. Email:wzshen@sjtu.edu.cn
2005-10-24 收到,2006-01-16 定稿